Inorganic Chemistry
Article

Inorg. Chem. **2009**, *48*, 11525–11532 **11525**
DOI: 10.1021/ic900809b

Luminescence Properties and Energy Transfer of Site-Sensitive $Ca_{6-x-y}Mg_{x-z}(PO_4)_4:Eu_y^{2+},Mn_z^{2+}$ Phosphors and Their Application to Near-UV LED-Based White LEDs

Ki Hyuk Kwon,[†,⊥] Won Bin Im,[‡,⊥] Ho Seong Jang,[§] Hyoung Sun Yoo,[†] and Duk Young Jeon*[,†]

[†]*Department of Materials Science and Engineering, Korea Advanced Institute of Science and Technology, Daejeon 305-701, Republic of Korea,* [‡]*Solid State Lighting and Energy Center, Materials Department, and Materials Research Laboratory, University of California, Santa Barbara, California 93106-5121, and* [§]*Department of Chemistry, Purdue University, West Lafayette, Indiana 47907.* [⊥] *The authors made equal contributions to this work.*

Received April 27, 2009

On the basis of the structural information that the host material has excellent charge stabilization, blue-emitting $Ca_{6-x-y}Mg_x(PO_4)_4:Eu_y^{2+}$ (CMP:Eu^{2+}) phosphors were synthesized and systematically optimized, and their photoluminescence (PL) properties were evaluated. Depending upon the amount of Mg added, the emission efficiency of the phosphors could be enhanced. The substitution of Eu^{2+} affected their maximum wavelength (λ_{max}) and thermal stability because the substitution site of Eu^{2+} could be varied. To obtain single-phase two-color-emitting phosphors, we incorporated Mn^{2+} into CMP:Eu^{2+} phosphors. Weak red emission resulting from the forbidden transition of Mn^{2+} could be enhanced by the energy transfer from Eu^{2+} to Mn^{2+} that occurs because of the spectral overlap between the photoluminescence excitation (PLE) spectrum of Mn^{2+} and the PL spectrum of Eu^{2+}. The energy transfer process was confirmed by the luminescence spectra, energy transfer efficiency, and decay curve of the phosphors. Finally, the optimized $Ca_{6-x-y}Mg_{x-z}(PO_4)_4:Eu_y^{2+},Mn_z^{2+}$ (CMP:Eu^{2+},Mn^{2+}) phosphors were applied with green emitting $Ca_2MgSi_2O_7:Eu^{2+}$ (CMS:Eu^{2+}) phosphors to ultraviolet (UV) light emitting diode (LED)-pumped white LEDs. The CMS:Eu^{2+}-mixed CMP:Eu^{2+}, Mn^{2+}-based white LEDs showed an excellent color rendering index (CRI) of 98 because of the broader emission band and more stable color coordinates than those of commercial $Y_3Al_5O_{12}:Ce^{3+}$ (YAG:Ce^{3+})-based white LEDs under a forward bias current of 20 mA. The fabricated white LEDs showed very bright natural white light that had the color coordinate of (0.3288, 0.3401), and thus CMP:Eu^{2+},Mn^{2+} could be regarded as a good candidate for UV LED-based white LEDs.

1. Introduction

Commercial white light emitting diodes (white LEDs) offer advantages such as low power consumption, long lifetime (> 100 000 h), and environmental friendliness and are fabricated by combining a blue LED chip with yellow-emitting phosphor.[1] Although commercial blue-LED-pumped, yellow-emitting phosphor-based white LEDs have high efficiency (> 30 lm/W), they have a poor color rendering index (< 65) because of weak red emission. Furthermore, most phosphors have no absorption band in the range from 440 to 460 nm with the exception of the commercial yellow phosphor, $Y_3Al_5O_{12}:Ce^{3+}$. Recently, a new class of white LEDs, i.e., near-ultraviolet LEDs (near-UV LEDs) combined with multiphase phosphors, have been developed to provide excellent color-rendering properties compared to those of commercial white LEDs.[2]

However, this new type of white LED has low luminescence efficiency because of the reabsorption of blue emission by red and green phosphors; there is also a high cost issue to produce such devices.[3] In studies on phosphors, numerous researchers have studied the energy transfer mechanism between two activators.[3−5] One activator, serving as a sensitizer, helps another activator to emit efficiently, and the two activators simultaneously substitute one host lattice to form single-phase and multicolor-emitting phosphors. Furthermore, a single-phase emitting phosphor utilizing energy transfer in the phosphor can be advantageous for

*To whom correspondence should be addressed. Fax: +82-42-350-3310 Tel: +82-42-350-3337 E-mail: dyj@kaist.ac.kr.

(1) Nakamura, S.; , Fasol, G., *The Blue Laser Diode*; Springer: Berlin, 1996.
(2) Uchida, Y.; Taguchi, T. *Opt. Eng.* **2005**, *44*(12), 124003.
(3) Won, Y. H.; Jang, H. S.; Im, W. B.; Lee, J. S.; Jeon, D. Y. *Appl. Phys. Lett.* **2006**, *89*, 231909.
(4) Shinn, M. D.; Sibley, W. A. *Phys. Rev. B* **1984**, *29*, 7.
(5) Kim, J. S.; Jeon, P. E.; Park, Y. H.; Choi, J. C.; Park, H. L.; Kim, G. C.; Kim, T. W. *Appl. Phys. Lett.* **2004**, *85*, 3696.

Published on Web 11/20/2009

near-UV LEDs-based white LEDs due to the following reasons. In this case, there is no reabsorption of blue emission and there is no need to mix two or three different phosphors. Consequently, this single-phase emitting phosphor can enhance the luminescence efficiency and color reproducibility of the white light source.

Phosphors based on phosphates have distinctive characteristics such as excellent thermal stability and stabilization of ionic charge in the lattice compared to other oxide phosphors.[6] B. Dickens et al. reported on the crystal structural information on $Ca_7Mg_9(Ca_{2-x},Mg_x)(PO_4)_{12}$.[7] They reported that this composition can be easily changed to several compositions having different stoichiometry in terms of the variable ratio between Ca and Mg, and $Ca_{6-x}Mg_x(PO_4)_4$ (CMP) is also a variation of the original composition. CMP was selected as a basic composition because CMP:Eu^{2+} phosphor has good luminescence properties under near-UV excitation.[8] R. A. McCauley et al. reported the influence of Mg content in the CMP:Eu^{2+} phosphor.[8] They explained that a solid solution of CMP between $Ca_3(PO_4)_2$ and $Mg_3(PO_4)_2$ can be formed in Mg content range of 2.76−3.6 mol and its luminescence properties are enhanced with increasing Mg content in this range. From this information, the influence of Mg content was studied in the present paper, as no scientific basis for its ameliorating effect was provided in the previous research. The crystal structure of CMP is monoclinic and its space group is $C2/c$. In the lattice of CMP, there are five different Ca sites that can be substituted by Eu^{2+} as an activator. Each Ca site has different structural information such as coordination number (n), which mainly affects the environment of the activators. Thus, the CMP-based phosphor will show site-sensitive characteristics on which the luminescence properties and thermal stability can be dependent, because Eu^{2+} and a variable amount of Mg tend to substitute for the same Ca sites.

Furthermore, Mn^{2+} codoped CMP:Eu^{2+}, a single-phase, two-color-emitting phosphor, emitted blue and red radiation originating from Eu^{2+} and Mn^{2+}, respectively. Although the absorption and emission of Mn^{2+} are weak due to its forbidden transition, the emission of Mn^{2+} was considerably improved by the energy transfer from Eu^{2+} to Mn^{2+}. Furthermore, the energy-transfer mechanism was confirmed by the change in the luminescence spectra, energy-transfer efficiency, and decay curve of the phosphors. Finally, the generation of white color and fabrication of white LEDs by incorporating CMP:Eu^{2+},Mn^{2+} phosphor as well as its luminescent properties will be discussed.

2. Experimental Section

2.1. Synthesis. Powder samples of $Ca_{6-x-y}Mg_x(PO_4)_4$:Eu_y^{2+}, $Ca_{6-x-y}Mg_{x-z}(PO_4)_4$:$Eu_y^{2+}$,$Mn_z^{2+}$ were prepared by a conventional solid-state reaction method. To synthesize the phosphor samples, we used $CaHPO_4$ (Aldrich, 98.0+ %), MgO (Aldrich, 99.99%), $(NH_4)_2HPO_4$ (Aldrich, 99.99%), Eu_2O_3 (Aldrich, 99.99%), and MnO (Aldrich, 99.99%) as raw materials. After the raw materials were mixed using an agate mortar for 1 h with ethanol, the mixed raw materials were dried at 85 °C for 1 h. Finally, the samples were sintered at 1100 °C for 5hrs in a reducing atmosphere of H_2 (5%) and N_2 (95%).

2.2. Characterizations. To investigate its luminescent properties, we characterized photoluminescence (PL) and photoluminescence excitation (PLE) with a DARSA PRO 5100 PL system (Professional Scientific Instrument Co., Korea) using a xenon lamp (500W) as an excitation source. The crystal structures of the samples were investigated by X-ray diffraction (XRD) patterns obtained by a Rigaku diffractometer with Cu Kα radiation (λ = 1.54 Å). To obtain lattice parameters, we employed the LeBail pattern-matching method, as implemented in the General Structure Analysis System (GSAS) program.[9]

2.3. Fabrication of White LEDs. To fabricate white LEDs, we combined UV LED chips (λ_{max} = 380−385 nm, nonepoxy molding packages and lamp type LEDs, TEKCORE Co., Ltd., TAIWAN) with CMP:Eu^{2+},Mn^{2+} phosphors and yellowish-green emitting $Ca_2MgSi_2O_7$:Eu^{2+} (CMS:Eu^{2+}) phosphors. Optical properties such as luminescence spectra, luminous efficiency, color-rendering index, and the Commission Internationale de l'Eclairage (CIE) color coordinates of the initial mixed phosphors and the white LEDs fabricated were characterized using a DARSA PRO 5100 PL system (PSI Trading Co. Ltd., Korea) and evaluated under a forward bias current of 20 mA at room temperature.

3. Results and Discussion

3.1. Luminescent Properties of Optimized CMP:Eu^{2+} Phosphors. We have synthesized the monoclinic phase of CMP:Eu^{2+} at 1100 °C successfully. The XRD pattern of the sample agrees well with JCPDS 73−1182, which correspond to monoclinic CMP. The obtained lattice parameters of $Ca_{2.94}Mg_3(PO_4)_4$:$Eu_{0.06}^{2+}$ were a = 22.9496 Å, b = 9.8605 Å, c = 16.9674 Å, β = 99.86° by LeBail pattern-matching of powder X-ray diffraction profile (R_{wp} = 13.54−14.09%). Although Eu^{2+} substituted for Ca sites, there is no significant change in the XRD patterns compared to that of the JCPDS card and the simulated XRD patterns. This indicates that the phosphor samples were well-synthesized by the solid-state reaction method and have high crystallinity.

In the lattice of CMP, the ionic radius of Ca is about 1.00 Å (n = 6), 1.06 Å (n = 7), and 1.12 Å (n = 8), whereas the ionic radius of Mg is about 0.72 Å (n = 6) and the valence of P is +5. Here, n denotes the coordination number of an ionic site. Judging from this information, Eu^{2+} (n = 8, 1.2 Å) will likely substitute a Ca site having similar ionic size and the same valence as an activator. To evaluate the basic luminescent properties of CMP:Eu^{2+} phosphor, the PL and PLE spectra of 0.06 mol of Eu^{2+}-doped CMP phosphor were recorded at room temperature. Figure 1 shows the photoluminescence (PL) and photoluminescence excitation (PLE) spectra of $Ca_{5.94-x}Mg_x(PO_4)_4$:$Eu_{0.06}^{2+}$ phosphor with various Mg content. As shown in Figure 1, the spectra of phosphor show a strong absorption band in the UV region ascribed to the transition from $^8S_{7/2}$ to e_g and t_{2g}, and a blue emission ascribed to the transition from t_{2g} to $^8S_{7/2}$. PLE and PL intensity enhanced with increasing Mg content. This result is consistent with expectations based on previous research results.[8] Critical evidence that can show the change of interaction among Eu^{2+} ions depending upon

(6) Tang, Y. S.; Hu, S. F.; Lin, C. C.; Bagkar, N. C.; Liu, R. S. *Appl. Phys. Lett*. **2007**, *90*, 151108.
(7) Dickens, B.; Brown, W. E. *Mineral. Petrogr. Mitt*. **1971**, *16*, 1.
(8) McCauley, R. A.; Hummel, F. A.; Hoffman, M. V. *J. Electrochem. Soc*. **1971**, *118*, 5.
(9) Blasse, G. *Philips Res. Rep*. **1969**, *24*, 131.

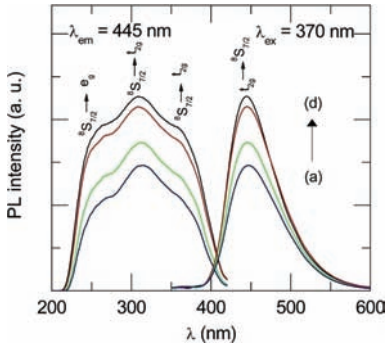

Figure 1. PLE and PL spectra of $Ca_{5.94-x}Mg_x(PO_4)_4:Eu_{0.06}^{2+}$ with Mg contents of (a) 2.76, (b) 3.0, (c) 3.3, and (d) 3.6 mol.

Table 1. Various Luminescence Properties of $Ca_{6-x-y}Mg_x(PO_4)_4:Eu_y^{2+}$

Mg content (x moles)	critical conc. (y moles)	critical distance (Å)	variation of λ_{em} (nm)
2.76	0.07	27.568	450
3.0	0.09	25.327	445
3.6	0.10	24.410	438

various Mg content is needed, as the present PL results are not sufficient to explain the influence of Mg content.

To confirm the fact that the PL intensity increases with increasing Mg contents, the critical concentration and critical distances where concentration quenching occurred were calculated for each case, i.e. for Mg = 2.76, 3.0, and 3.6 mol. Table. 1 shows the critical concentration and critical distance[10] for each case. When the phosphor samples were systematically synthesized with varying Mg content, the critical concentrations increased and critical distances decreased with increasing Mg content. This means that concentration quenching occurs at high Eu^{2+} concentration and a large amount of Eu^{2+} can substitute for Ca site in the case of high Mg content. Thus, its PL intensity was superior to that of other cases, and this result is consistent with the observations of the PL and PLE spectra.

The basis of the structural information,[8] five different Ca sites that can be substituted by Eu^{2+} and Mg can be classified into three groups based upon their coordination number, i.e., 8-coordinated site, 7-coordinated site and 6-coordinated site. In $Ca_3Mg_3(PO_4)_4$ host lattice, there are 36 Ca sites in one unit cell. Among 36 Ca sites, the number of 6-, 7-, and 8-coordinated Ca sites is 8, 8 and 20, respectively. Therefore, when Eu^{2+} substitutes a Ca site in the CMP, Eu substitutes 6-coordinated, 7-coordinated, and 8-coordinated Ca sites in a ratio of 2: 2: 5. Generally, Eu^{2+} ions substitute for Ca sites by this ratio because the ionic radius of Eu^{2+} is slightly larger than that of Ca. However, it is expected that Mg (n = 6, 0.86 Å) tends to substitute first the 6-coordinated Ca site (n = 6, 1.14 Å), which has a small size difference from Mg, because the ionic size of Mg is much smaller than that of Ca. For this reason, Eu^{2+} might substitutes for the Ca site in a different ratio where there is a high rate of high-coordinated Ca sites with increasing Mg content rather than the ratio noted above. This assumption can be confirmed by

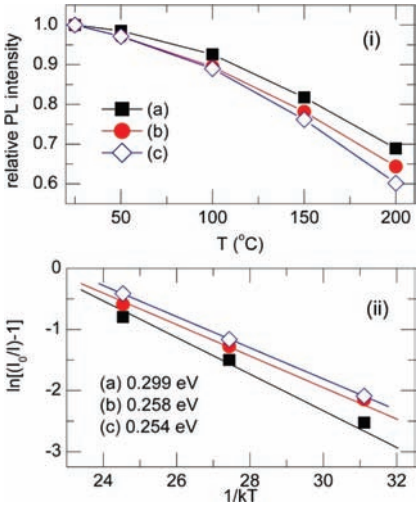

Figure 2. (i) PL results of $Ca_{5.92-x}Mg_x(PO_4)_4:Eu_{0.08}$ phosphor samples with Mg content of (a) 2.76, (b) 3.0, and (c) 3.6 mol at various 2nd heat-treatment temperatures. (ii) The activation energy of thermal quenching of $Ca_{5.92-x}Mg_x(PO_4)_4:Eu_{0.08}$ phosphor samples with Mg content.

the following results on the variation of emission wavelengths. As shown in Table 1, the emission wavelength moves to shorter wavelength with increasing Mg content. This phenomenon can be explained by a crystal field effect.[11]

Each Ca site has different structural information. Hence, it is expected that each Ca site will have different thermal stability. Figure 2i shows the PL results of phosphor samples with various Mg concentrations at various second heat treatment temperatures in a range from room temperature to 200 °C. In the case of Mg content (Mg = 2.76), the decreased amount of emission intensity is smaller than those of other cases. On the other hand, when the Mg content is low, the phosphor has better thermal stability than those in other cases. This phenomenon can be explained by Pauling's second rule.[12] Among the five rules, the second rule explains that the bond valence, called the electrostatic strength, of each ion should be approximately equal to its oxidation state. On the other hand, the valence of an ion (V_i equal to the oxidation state of the ion, and S equal to the number of coordination) is equal to the sum of the valences of its bonds (s_{ij}). Therefore, this explanation can be expressed by the following relation.

$$V_i = S \times S_{ij} \quad (1)$$

The electrostatic strength of each Ca site was calculated by this relation. The electrostatic strengths of 6-, 7-, and 8-coordinated Ca site are approximately +0.3333, +0.2857, and +0.2500, respectively. Therefore, the low-coordinated Ca site will have large electrostatic strength and Eu^{2+}, which substitutes low-coordinated Ca sites, will have high thermal stability against external influences. Therefore, Eu^{2+} can likely substitute greater amounts of low-coordinated Ca sites in the case of Mg concentration (Mg = 2.76) and shows good thermal stability. On the basis of these results, the activation energy of

(10) Larson, A. C.; Von Dreele, R. B. *GSAS. General Structure Analysis System Program and Handbook*; Los Alamos National Laboratory Report LAUR 86-748; Los Alamos National Laboratory: Los Alamos, NM, **1994**.

(11) Blasse, G. *J. Solid State Chem.* **1986**, *62*, 207.
(12) Im, W. B.; Kim, Y.-I.; Jeon, D. Y. *Chem. Mater.* **2006**, *18*, 1190–1195.

thermal quenching was calculated by the Arrhenius equation, which has been used to calculate the activation energy.[6,13]

$$I(T) \approx \frac{I_0}{1 + c\,\exp\left(\frac{-E}{kT}\right)} \quad (2)$$

where $I(T)$ is the intensity at a given temperature, I_0 is the initial intensity, c is a constant, k is Boltzman's constant, T is temperature, and E is activation energy.

Figure 2ii shows the activation energy of thermal quenching of phosphor samples with various Mg content, calculated by the Arrhenius equation. In the case of Mg contents (Mg = 2.76), the phosphor is expected to show good thermal stability because of its high activation energy. From the results shown in Figure 2, the behavior of substitution of Eu^{2+} and Mg for Ca sites was also well-noticed by these results and was consistent with the assumption described above.

3.2. Energy Transfer from Eu^{2+} to Mn^{2+} in the CMP. Mn^{2+} has weak red emission because of its forbidden transition required by the selection rule.[14] Mn^{2+} can show various emission wavelengths because of the influence of the crystal field against the external crystal field.[3] In the case of CMP:Eu^{2+},Mn^{2+} phosphor, Mn^{2+} easily substitutes the Mg site because of its similarity in ionic size and valence. Therefore, the Mg site that can be substituted by Mn^{2+} was evaluated, because the external crystal field affects the emission wavelength of Mn^{2+}. Although there are five different Mg sites in the CMP, almost all sites are coordinated with 6 oxygens.[7] Therefore, when Mn^{2+} substitutes the Mg site in the CMP, we can expect that Mn^{2+} will show red emission. Figure 3i shows the PLE and PL spectra of CMP:Mn^{2+} phosphor. As shown in this figure, the excitation of Mn^{2+} is due to the transitions of $^6S_0 \rightarrow {}^4T_2(^4F)$, $^6S_0 \rightarrow {}^4T_1(^4F)$, $^6S_0 \rightarrow {}^4E(^4D)$, $^6S_0 \rightarrow {}^4T_2(^4D)$, and $^6S_0 \rightarrow {}^4G$ and the weak red emission is due to the transition of $^4T_1 \rightarrow {}^6A_1$.[15,16] As expected, Mn^{2+} in the Mg site of CMP shows very weak red emission. To confirm the energy transfer from Eu^{2+} to Mn^{2+} and the role of Eu^{2+} as a sensitizer, the PL spectrum of CMP:Eu^{2+} and PLE spectrum of CMP:Mn^{2+} have to overlap with each other.[17−19] Figure 3ii shows the PLE spectrum of Mn^{2+} and PL spectrum of Eu^{2+}. One can expect that the energy absorbed by Eu^{2+} can transfer to Mn^{2+} because of the spectral overlap in the region of 400−450 nm. The PLE intensity (Mn^{2+}) of CMP:Eu^{2+},Mn^{2+} increases compared to that of CMP:Mn^{2+}. Also, the spectral shape PLE of CMP:Eu^{2+},Mn^{2+} has the spectral shapes PLE of both CMP:Eu^{2+} and CMP:Mn^{2+} (see Figure 3iii). Hence, Eu^{2+} and also Mn^{2+} incorporated

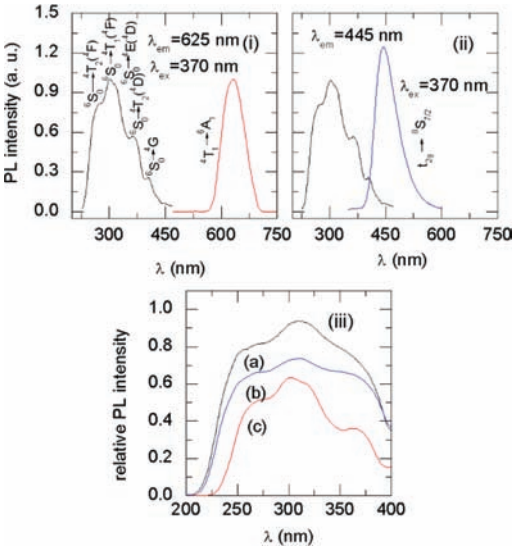

Figure 3. (i) PLE and PL spectra of $Ca_{2.4}Mg_{3.54}(PO_4)_4$:$Mn_{0.06}{}^{2+}$ phosphor. (ii) PLE spectrum of $Ca_{2.4}Mg_{3.54}(PO_4)_4$:$Mn_{0.06}{}^{2+}$ and PL spectrum of $Ca_{2.34}Mg_{3.6}(PO_4)_4$:$Eu_{0.06}{}^{2+}$. (iii) PLE spectra of (a) $Ca_{2.34}Mg_{3.6}(PO_4)_4$:$Eu_{0.06}{}^{2+}$, (b) $Ca_{2.4}Mg_{3.54}(PO_4)_4$:$Mn_{0.06}{}^{2+}$, and (c) $Ca_{2.34}Mg_{3.54}(PO_4)_4$:$Eu_{0.06}{}^{2+}$,$Mn_{0.06}{}^{2+}$ phosphors.

with CMP well and improvement of the luminescent properties of Mn^{2+} could be expected because of the energy transfer from Eu^{2+} to Mn^{2+}.

Figure 4i, ii shows the PL spectra of the phosphor samples prepared with a fixed Eu^{2+} concentration and varied Mn^{2+} concentration. Although the concentration of Eu^{2+} was fixed, the emission intensity of Eu^{2+} decreased with increasing Mn^{2+} concentration. Figure 4iii, iv shows the PL spectra of phosphor samples prepared with fixed Mn^{2+} concentration and varied Eu^{2+} concentration. Although the concentration of Mn^{2+} was fixed, the emission intensity of Mn^{2+} dramatically increased with increasing Eu^{2+} concentration. From these results, we can be sure about the efficient energy transfer from Eu^{2+} to Mn^{2+}. In the observation of the relative PL intensity of $Ca_{2.4-y}Mg_{3.6}(PO_4)_4$:$Eu_y{}^{2+}$ and $Ca_{2.4-y}$-$Mg_{3.54}(PO_4)_4$:$Eu_y{}^{2+}$,$Mn_{0.06}{}^{2+}$ phosphors, the two kinds of spectra show that the blue emission intensity of Eu^{2+} increases with increasing Eu^{2+} concentration. However, they show a difference in emission intensity and the difference is almost uniform for each case of Eu^{2+} concentration. This indicates that a certain amount of energy is absorbed by Eu^{2+} transferred to Mn^{2+}, which was of fixed concentration. Generally, the energy transfer efficiency from a sensitizer to activator can be expressed as the following equation[14]

$$\eta_T = 1 - \frac{I_S}{I_{S0}} \quad (3)$$

where η_T is the energy transfer efficiency and I_{S0} and I_S are the luminescence intensity of a sensitizer in the absence and presence of an activator, respectively. In this case, Eu^{2+} acts as a sensitizer and Mn^{2+} acts as an activator. Figure 5a shows the results of energy transfer efficiency from Eu^{2+} to Mn^{2+} calculated by eq 3 and Figure 5b is the trend of increasing emission intensity of Mn^{2+}. As shown in Figure 5a, the energy transfer efficiency increases with increasing Mn^{2+} concentration.

(13) Xie, R. J.; Hirosaki, N.; Kimura, N.; Sakuma, K.; Mitomo, M. *Appl. Phys. Lett*. **2007**, *90*, 191101.
(14) Yang, W. J.; Chen, T. M. *Appl. Phys. Lett*. **2006**, *88*, 101903.
(15) Wang, L.; Liu, X.; Hou, Z.; Li, C.; Yang, P.; Lin, J. *J. Phys. Chem. C* **2008**, *112*(48), 18882–18888.
(16) Kong, D. Y.; Yu, M.; Lin, C. K.; Liu, X. M.; Lin, J.; Fang, J. *J. Electrochem. Soc*. **2005**, *152*(9), H146–H151.
(17) Yao, G. Q.; Lin, J. H.; Zhang, L.; Lu, G. X.; Gong, M. L.; Su, M. Z. *J. Mater. Chem*. **1998**, *8*, 585.
(18) Yang, W. J.; Luo, L. Y.; Chen, T. M.; Wang, N. S. *Chem. Mater*. **2005**, *17*, 3883.
(19) Kim, J. S.; Jeon, P. E.; Choi, J. C.; Park, H. L.; Mho, S. L.; Kim, G. C. *Appl. Phys. Lett*. **2004**, *84*, 2931.

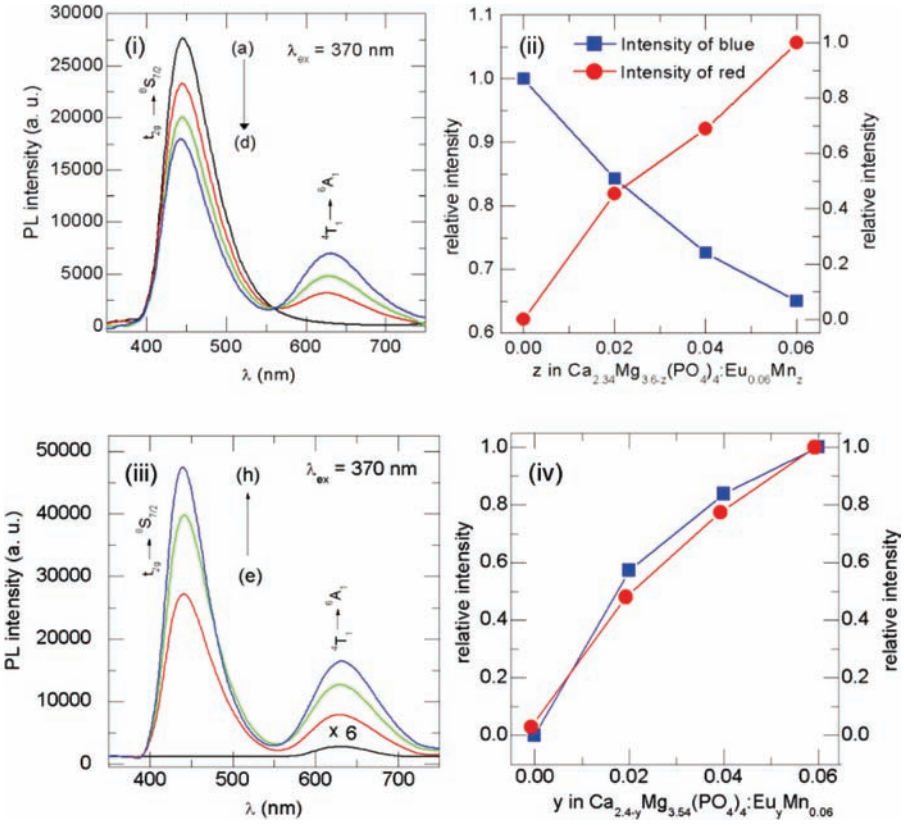

Figure 4. (i, ii) PL results of $Ca_{2.34}Mg_{3.6-z}(PO_4)_4:Eu_{0.06}^{2+},Mn_z^{2+}$ phosphors with (a) $z = 0$, (b) $z = 0.02$, (c) $z = 0.04$, (d) $z = 0.06$. (iii, iv) PL results of $Ca_{2.4-y}Mg_{3.54}(PO_4)_4:Eu_y^{2+},Mn_{0.06}^{2+}$ phosphors with (e) $y = 0$, (f) $y = 0.02$, (g) $y = 0.04$, (h) $y = 0.06$.

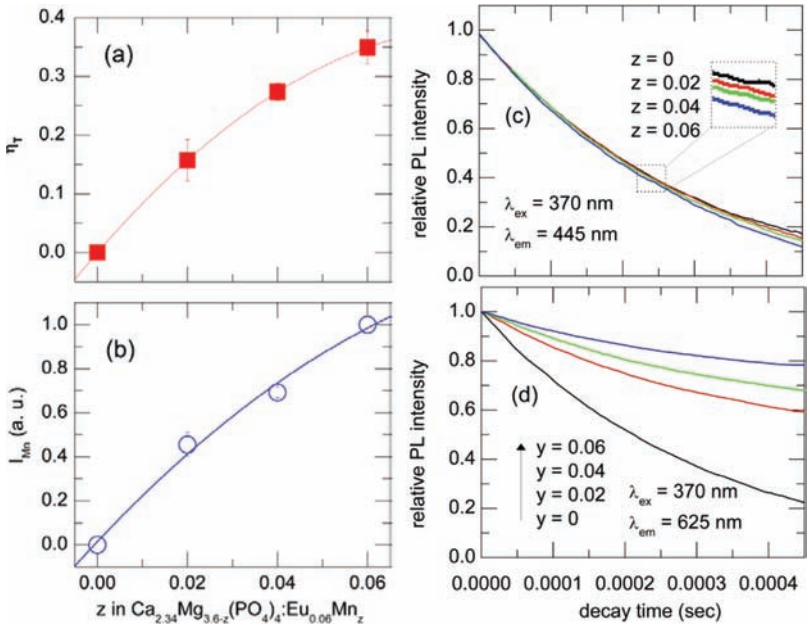

Figure 5. (a) Energy transfer efficiency from Eu^{2+} to Mn^{2+} in $Ca_{2.34}Mg_{3.6-z}(PO_4)_4:Eu_{0.06}^{2+},Mn_z^{2+}$; (b) trend of increasing emission intensity of Mn^{2+} in $Ca_{2.34}Mg_{3.6-z}(PO_4)_4:Eu_{0.06}^{2+},Mn_z^{2+}$. (c) Decay curve of Eu^{2+} in $Ca_{2.34}Mg_{3.6-z}(PO_4)_4:Eu_{0.06}^{2+},Mn_z^{2+}$, and (d) Mn^{2+} in $Ca_{2.4-y}Mg_{3.54}(PO_4)_4:Eu_y^{2+}$, $Mn_{0.06}^{2+}$.

However, the rate of increase of the emission intensity gradually decreases with increasing Mn^{2+} concentration. This indicates that the quantity of energy that can transfer from Eu^{2+} to Mn^{2+} is gradually restricted with increasing Mn^{2+} concentration, because the concentration of Eu^{2+} is fixed. This trend is similar to that of the results portrayed in the graph in Figure 5b. Therefore, efficient energy transfer from Eu^{2+} to Mn^{2+} can be expected from these results. Panels c and d in Figure 5 show the decay curve of Eu^{2+} and Mn^{2+}, respectively. The decay time of Eu^{2+} decreases with increasing Mn^{2+} concentration, and the decay time of Mn^{2+} increases with increasing Eu^{2+}

concentration. The decay time of Eu^{2+} decreases with increasing Mn^{2+} concentration because the energy absorbed by Eu^{2+} transferred to Mn^{2+}. In contrast, the decay time of Mn^{2+} increases with increasing Eu^{2+} concentration because Mn^{2+} absorbed the energy from Eu^{2+}. Thus, these results also indicate that energy transfer occurs efficiently from Eu^{2+} to Mn^{2+}.

According to Dexter and Schulman, concentration quenching is in many cases due to energy transfer from one activator to another until an energy sink in the lattice is reached.[20] As suggested by Blasse,[9] the average separation R_{Eu-Mn} can be expressed by

$$R_{Eu-Mn} = 2\left[\frac{3V}{4\pi xN}\right]^{1/3} \quad (4)$$

where N is the number of Z ions in the unit cell, and V is the volume of the unit cell. For $Ca_3Mg_3(PO_4)_4$ host, $N = 36$ and $V = 3839.63$ Å^3. x is the total concentration of Eu^{2+} and Mn^{2+}. Thus, R_{Eu-Mn} (in Å) is determined to be 13.66, 12.68, and 11.93, corresponding to 0.02, 0.04, and 0.06 in $Ca_{2.94}Mg_{3-z}(PO_4)_4$:$Eu_{0.06}$,$Mn_z$. It turns out that the critical concentration x_c was 0.14 at which the luminescence intensity of Eu^{2+} is only half of that of the sample with no Mn^{2+} included. Therefore, the critical distance (R_c) of energy transfer was calculated to be about 11.33 Å. We have also observed that the radiative emission from Eu^{2+} prevails when $R_{Eu-Mn} > R_c$ and energy transfer from Eu^{2+} to Mn^{2+} dominates when $R_{Eu-Mn} < R_c$.

The energy transfer mechanism between Eu^{2+} and Mn^{2+} in CMP:Eu^{2+},Mn^{2+} should be controlled by electric multipole−multipole interaction according to Dexter theory, which follows the energy transfer equation given below[18,22,23]

$$\frac{I_{S0}}{I_S} \propto C^{n/3} \quad (5)$$

where I_{S0} is the intrinsic luminescence intensity of Eu^{2+} and I_S is the luminescence intensity of Eu^{2+} in the presence of the Mn^{2+}. The $n = 6$, 8, or 10 are dipole−dipole, dipole−quadrupole, or quadrupole−quadrupole interactions, respectively. The value of n can be determined from the slop (n/3) of the linear line in Figure 6 which plots log (I/C) vs log(C) on a logarithmic scale of I/C. The value of n/3 is found to be 5.808. Therefore, the value of n is calculated approximately 6. This indicates that dipole−dipole interaction is the energy transfer mechanism between Eu^{2+} and Mn^{2+} in the CMP:Eu^{2+}, Mn^{2+} phosphor.

3.3. Fabrication of White LEDs by Including CMP:Eu^{2+},Mn^{2+} Phosphors. To fabricate white LEDs with a high color rendering index, blue and red emitting CMP:Eu^{2+},Mn^{2+} phosphors were combined with yellowish-green emitting phosphors, CMS:Eu^{2+}. Figure 7 shows the PL spectra and color coordinates of CMS:Eu^{2+}-mixed

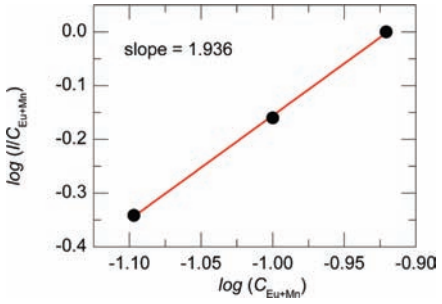

Figure 6. Logarithm of the emission intensity per activator ion (log I/C_{Eu+Mn}) as a function of logarithm of the ($Eu^{2+} + Mn^{2+}$) concentration (log C_{Eu+Mn}) in CMP:Eu^{2+},Mn^{2+} phosphor.

CMP:Eu^{2+},Mn^{2+} phosphors with various ratios between the amount of CMP:Eu^{2+},Mn^{2+} and that of CMS:Eu^{2+} phosphors, respectively. As shown in Figure 7a−c, each phosphor has a broad emission band in the wide region of wavelength and high color rendering index (CRI), i.e., (a) $R_a = 82$, (b) $R_a = 88$, and (c) $R_a = 86$, respectively. As shown in Figure 7d, the color coordinates of the phosphor samples as well as the color rendering index could be tuned by the ratio between the amount of CMP:Eu^{2+}, Mn^{2+} and that of CMS:Eu^{2+}. The phosphor samples were coated onto UV LED chips with a maximum excitation wavelength of 380−385 nm. Figure 7e shows photographs of emission from CMS:Eu^{2+}-mixed CMP:Eu^{2+},Mn^{2+} phosphor with a mixture ratio of 8:1-based white LEDs under a forward bias current of 20 mA, which generally commercial white LEDs are operated at 20 mA.[21] The CMP:Eu^{2+},Mn^{2+} and CMS:Eu^{2+}-based white LEDs generated bright white light at 20 mA.

Figure 8i shows electroluminescence (EL) spectra of the CMS:Eu^{2+}-mixed CMP:Eu^{2+},Mn^{2+} -based white LEDs. Three emission bands were clearly located at ~460, ~535, and 620 nm, respectively. When the PL spectra of initial phosphor samples were compared to the EL spectra of this white LEDs, the blue emission generated by Eu^{2+} from CMP:Eu^{2+},Mn^{2+} moved to longer wavelength and red emission generated by Mn^{2+} from CMP:Eu^{2+},Mn^{2+} increased. In this regard, the EL properties of phosphor depend on the packaging condition such as the amount of phosphor coating on the LED chip because of the red-shift caused by the reabsorption.[24] In particular, The CMS:Eu^{2+}-mixed CMP:Eu^{2+},Mn^{2+} -based white LEDs operated at 20 mA showed natural white light with color coordinates of (0.3288, 0.3401), a color temperature (T_c) of 6066 K, and an excellent CRI (R_a) of 98. Figure 8ii shows the CRI of the optimized white LED under a forward bias current of 20 mA. The general CRI is designated by the symbol R_a, which is the average value of R1 to R8.[21] The numbers in parentheses indicate the Munsell color system.[22] A commercial $Y_3Al_5O_{12}$:Ce^{3+} (YAG:Ce^{3+})-based white LED having a R_a of 78 was compared to the CMS:Eu^{2+}-mixed CMP:Eu^{2+},Mn^{2+} -based white LED, and the latter showed higher R values. In particular, the values of R1 (7.5R) and R8 (10P) related to red emission are higher than those of the commercial YAG:Ce^{3+}-based white LED, which has weak red emission. Furthermore,

(20) Dexter, D. L.; Schulman, J. A. *J. Chem. Phys.* **1954**, *22*, 1063.
(21) Jang, H. S.; Yang, H.; Kim, S. W.; Han, J. Y.; Lee, S. −G.; Jeon, D. Y. *Adv. Mater.* **2008**, *20*, 2696–2702.
(22) Wyszecki, G.; , Stiles, W. S., *Color Science: Concepts and Methods, Quantitative Data and Formulae*, 2nd ed.; John Wiely & Sons: New York, 1982; Chapter 6.
(23) Van Uitert, L. G. *J. Electrochem. Soc.* **1967**, *114*, 1048.
(24) Sakuma, K.; Hirosaki, N.; Xie, R.-J. *J. Lumin.* **2007**, *126*, 843.

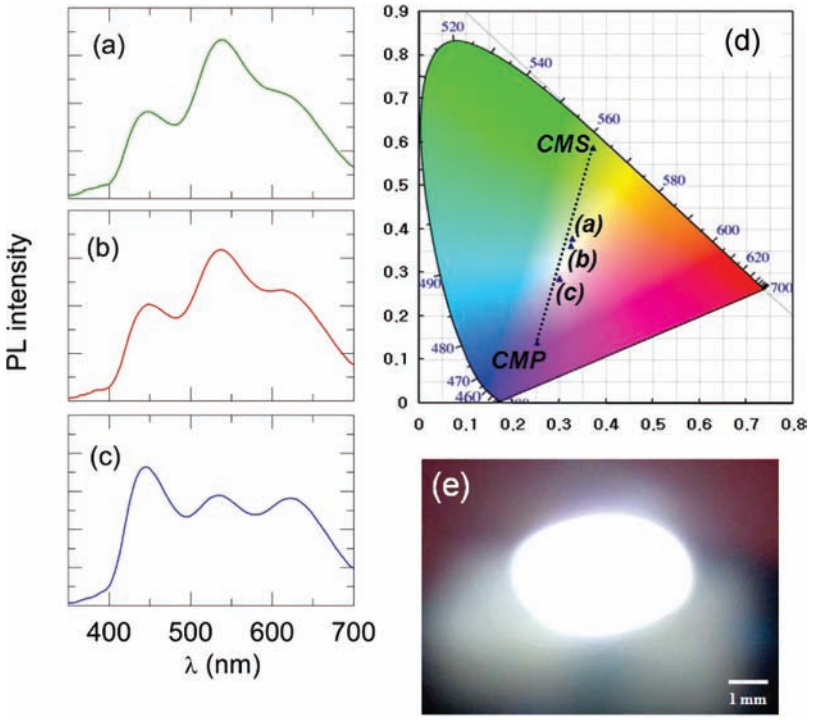

Figure 7. PL spectra of mixed phosphors with various ratios between the amount of $Ca_{2.34}Mg_{3.54}(PO_4)_4:Eu_{0.06}^{2+},Mn_{0.06}^{2+}$ and $Ca_{1.93}MgSi_2O_7:Eu_{0.07}^{2+}$ phosphors: (a) CMP:CMS = 1:1, (b) CMP:CMS = 4:1, and (c) CMP:CMS = 8:1. (d) Color coordinates of mixed phosphors with various ratios between the amount of $Ca_{2.34}Mg_{3.54}(PO_4)_4:Eu_{0.06}^{2+},Mn_{0.06}^{2+}$ and that of $Ca_{1.93}MgSi_2O_7:Eu_{0.07}^{2+}$ phosphors: (a) CMP:CMS = 1:1, (b) CMP:CMS = 4:1, and (c) CMP:CMS = 8:1. (e) Photograph of emission from $Ca_{2.34}Mg_{3.54}(PO_4)_4:Eu_{0.06}^{2+},Mn_{0.06}^{2+}$ and $Ca_{1.93}MgSi_2O_7:Eu_{0.07}^{2+}$ with a mixture ratio of 8:1-based white LEDs under a forward bias current of 20 mA.

R4 (2.5G) related to green emission is higher than that of the commercial YAG:Ce^{3+}-based white LED due to the addition of yellowish-green emitting CMS:Eu^{2+} phosphors.

As shown in Figure 8i, the EL intensity increased continuously with increasing applied forward bias current. This indicates that the CMS:Eu^{2+}-mixed CMP:Eu^{2+},Mn^{2+} -based white LED does not show spectral saturation and the mixed phosphors can be regarded as promising candidates for UV LED-based white LED applications. Although the R_a values of the CMS:Eu^{2+}-mixed CMP:Eu^{2+},Mn^{2+}-based white LED were changed from 98 at 20 mA to 92 at 40 mA, the R_a value is still higher than that of the commercial YAG:Ce^{3+}-based white LED. In addition, there is a very small difference between the color coordinates of (0.3288, 0.3401) at 20 mA and (0.3202, 0.3219) at 40 mA, indicating that the CMS:Eu^{2+}-mixed CMP:Eu^{2+},Mn^{2+}-based white LED has high color stability. Although the luminous efficacy of the fabricated white LEDs ($\sim$ 5.49 lm/W) was lower than that of commercial blue-LED-pumped, yellow-emitting phosphor-based white LEDs, the efficiency can be enhanced through further optimization of the luminescence properties of the phosphors and the fabrication process of the white LEDs. In particular, the efficiency of UV LED chips is still low, because UV LED-based white LEDs are under development. If efficient UV LEDs will be developed, the luminous efficacy can be significantly improved. The CMS:Eu^{2+}-mixed CMP:Eu^{2+},Mn^{2+} phosphors show excellent luminescence properties and the CMS:Eu^{2+}-mixed CMP:Eu^{2+},Mn^{2+}-based white LEDs also show better optical properties than those of commercial white LEDs.

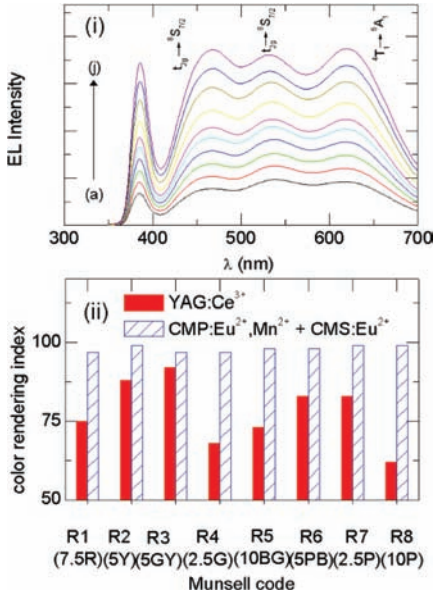

Figure 8. (i) EL spectra of the $Ca_{1.93}MgSi_2O_7:Eu_{0.07}^{2+}$-mixed $Ca_{2.34}Mg_{3.54}(PO_4)_4:Eu_{0.06}^{2+},Mn_{0.06}^{2+}$-based white LEDs under forward bias current of (a) 12, (b) 14, (c) 16, (d) 18, (e) 20, (f) 22, (g) 24, (h) 30, (i) 38, and (j) 40 mA. (ii) Color rendering indices of commercial YAG:Ce^{3+}-based white LED and $Ca_{1.93}MgSi_2O_7:Eu_{0.07}^{2+}$-mixed $Ca_{2.34}Mg_{3.54}(PO_4)_4:Eu_{0.06}^{2+},Mn_{0.06}^{2+}$-based white LED under a forward bias current of 20 mA.

4. Conclusion

To address issues such as reabsorption of blue emission and the costliness to produce white LED devices, a single-phase emitting phosphor is a promising candidate that results in enhancing the luminescence efficiency and color reproducibility

of the white light source. From this motivation, CMP:Eu^{2+}, Mn^{2+} phosphor was selected as a candidate. First, to prepare optimized CMP:Eu^{2+}, we evaluated its luminescent properties. CMP:Eu^{2+} can form a solid solution between $Ca_3(PO_4)_2$ and $Mg_3(PO_4)_2$ in a concentration range of Mg from 2.76 to 3.6 mol, as determined from the phase diagram. In this range, the emission intensity of CMP:Eu^{2+} increases with increasing Mg concentration because the critical concentration increases and the interaction among Eu^{2+} ions decreases with increasing Mg concentration. The emission wavelengths of phosphor samples prepared with various Mg concentrations move to the short wavelength with increasing Mg concentration. Also, in the case of low Mg concentration, the phosphor shows better thermal stability than that of other cases. To synthesize the single-phase, two-color-emitting phosphor via energy transfer from Eu^{2+} to Mn^{2+}, we also considered the luminescent properties of CMP:Eu^{2+},Mn^{2+} phosphor. Eu^{2+} was used as a sensitizer because of the weak red emission of Mn^{2+} originating from its forbidden transition in this system and two activators, Eu^{2+} and Mn^{2+}, were used to make a two color emitting phosphor. The energy transfer from Eu^{2+} to Mn^{2+} was confirmed by several experimental results such as the luminescence spectra, energy-transfer efficiency, and decay curve of the phosphors. To generate white color by using CMP:Eu^{2+},Mn^{2+} phosphor, this phosphor was combined with a yellowish-green phosphor (CMS:Eu^{2+}). The mixed phosphors showed a broad emission band in a wide region of emission wavelength and a high color rendering index. The CMP:Eu^{2+},Mn^{2+} and CMS:Eu^{2+}-based white LED exhibited an excellent color rendering index of 98, color coordinates of (0.3288, 0.3401), a color temperature of 6066 K, and bright natural white light under a forward bias current of 20 mA. Thus, this white LED is thought to be a promising white light source with high color rendering.

Supporting Information Available: Figures S1−S6 (PDF). This material is available free of charge via the Internet at http://pubs.acs.org.